Confinement of surface acoustic waves in AlN/GaN/γ-$LiAlO_2$ acoustic wells

Y. Takagaki[a)]
Paul-Drude-Institut für Festkörperelektronik, Hausvogteiplatz 5-7, 10117 Berlin, Germany

E. Chilla
Vectron International, Tele Filter, Potsdamer Strasse 18, 14513 Teltow, Germany

K. H. Ploog
Paul-Drude-Institut für Festkörperelektronik, Hausvogteiplatz 5-7, 10117 Berlin, Germany

(Received 26 July 2004; accepted 3 November 2004; published online 30 December 2004)

We numerically investigate the characteristics of surface acoustic waves (SAWs) in AlN/GaN/γ-$LiAlO_2$ heterostructures. The markedly large sound velocity in AlN in comparison to that in GaN leads to an expulsion of SAWs from the top AlN layer and their resultant relocation to the middle GaN layer in the short-wavelength regime. The SAW velocity in the limit of zero wavelength is given by a bulk sound velocity of GaN, owing to the capping by the AlN barrier layer. The extra confinement of the SAW power in the acoustic well is advantageous in manipulating the operation of GaN-based devices by SAWs. The threshold velocity for the appearance of guided Rayleigh-like modes is found to be smaller than the bulk transverse sound velocity in the substrate. The present system exhibits furthermore unusual bowing behavior in the SAW dispersion. © *2005 American Institute of Physics*. [DOI: 10.1063/1.1840103]

I. INTRODUCTION

Surface acoustic waves (SAWs) in AlN layers are of great interest for high-frequency applications because of their large velocity.[1–4] The strong electromechanical coupling in AlN is also crucial for SAW devices.[5,6] The devices will become further attractive if one can acoustically control the unique optical and electrical properties of GaN by embedding GaN-based quantum wells in the SAW propagation path. In designing such structures, one needs to take into account the modification of the SAW characteristics, resulting from the nonuniform sound velocities in the layered system.[7] AlN and GaN layers are typically grown on Al_2O_3(0001) and SiC(0001). A particular significance of the acoustic mismatch is observed for GaN layers on Al_2O_3 substrates[8] and AlN and GaN layers on SiC substrates.[9] Guided modes are generated in these cases as the SAW velocities in the top layers are smaller than those in the substrates.

Recently, the characteristics of SAWs have been investigated for AlN and GaN layers grown on γ-$LiAlO_2(10\bar{0})$.[10] The γ-$LiAlO_2$ substrates are utilized to have the $(1\bar{1}00)$ plane of hexagonal GaN and AlN layers designated to be the growth surface. The advantage of the *M*-plane orientation is the absence of built-in electrostatic fields in GaN–AlN quantum wells.[11] There exist giant fields when the quantum wells are *C* plane oriented, which is the case for the Al_2O_3(0001) and SiC(0001) substrates. The built-in fields are detrimental in incorporating the functionalities of GaN into SAW devices. They strongly quench the electron-hole recombination when the well width exceeds about 6 nm, thereby hindering the modulation of the optical properties by SAWs. In addition, a two-dimensional electron gas having a markedly large density is accumulated at the heterointerface due to the dipole charges, which screen the piezoelectric fields of SAWs. The *M*-plane quantum wells are free from these problems. We also note that the (Al,Ga)N/γ-$LiAlO_2$ heterostructures are suitable for microelectromechanical systems because of the nearly ideal etch selectivity between the III-nitrides and γ-$LiAlO_2$.[12]

In this paper, we numerically calculate the dispersion of SAWs in *M*-plane AlN–GaN bilayer films on γ-$LiAlO_2$(100). Our theoretical investigations are carried out for much wider parameter ranges than in the experiments of Ref. 10. The large velocity mismatch between AlN and GaN and the low crystal symmetry of γ-$LiAlO_2$ are shown to give rise to various unusual properties of SAWs in the parameter ranges that are not explored in the experiment.

II. NUMERICAL MODEL

Our model structure is illustrated in Fig. 1. The crystal structures of AlN and GaN are hexagonal, whereas γ-$LiAlO_2$ possesses a tetragonal crystal structure.

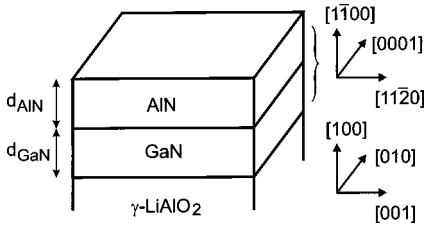

FIG. 1. Schematic of the AlN/GaN/γ-$LiAlO_2$ heterostructure. The thicknesses of the AlN and GaN layers are d_{AlN} and d_{GaN}, respectively. The crystal orientation relationship between the hexagonal AlN and GaN films and the tetragonal γ-$LiAlO_2$ substrate is shown on the right-hand side.

[a)]Electronic mail: takagaki@pdi-berlin.de

TABLE I. Mass density ρ (in units of 10^3 kg/m^3) and elastic stiffness constants c_{ij} (in units of 10^{11} N/m^2) of AlN, GaN, and γ-$LiAlO_2$. The nonzero elastic constants for the hexagonal and tetragonal crystal structures are $c_{1111}=c_{2222}=c_{11}$, $c_{1122}=c_{2211}=c_{12}$, $c_{1133}=c_{3311}=c_{2233}=c_{3322}=c_{13}$, $c_{3333}=c_{33}$, $c_{1313}=c_{1331}=c_{3113}=c_{3131}=c_{2323}=c_{2332}=c_{3223}=c_{3232}=c_{44}$, and $c_{1212}=c_{1221}=c_{2112}=c_{2121}=c_{66}$. Note that the hexagonal crystal structure of AlN and GaN enforces the relation $2c_{66}=c_{11}-c_{12}$.

	ρ	c_{11}	c_{12}	c_{13}	c_{33}	c_{44}	c_{66}
AlN	3.23	4.1	1.4	1	3.9	1.2	1.35
GaN	6.15	3.7	1.45	1.1	3.9	0.98	1.125
γ-$LiAlO_2$	2.64	1.2	0.59	0.6	1.5	0.7	0.7

$(1\bar{1}00)$-oriented AlN and GaN layers are assumed to be placed on the (100)-oriented surface of γ-$LiAlO_2$. The thicknesses of the AlN and GaN layers are d_{AlN} and d_{GaN}, respectively. Within the surface plane, the $[11\bar{2}0]$ and [0001] directions of the bilayer film are aligned along the [001] and [010] directions of the substrate, respectively.[11] That is, the c axes of the hexagonal and tetragonal crystals are orthogonal to each other in the interface plane. It ought to be noted that, due to the isotropic elastic properties within the C plane of hexagonal crystals, the results to be presented below are applicable, irrespective of the surface orientation of the AlN and GaN layers as long as their c axes lie in the surface plane as specified above.

The dispersion of SAWs in the AlN/GaN/γ-$LiAlO_2$ heterostructures is evaluated by numerically solving the wave equation

$$\sum_{i,k,l} c_{ijkl}\frac{\partial^2 u_k}{\partial x_l\,\partial x_i}=\rho\frac{\partial^2 u_j}{\partial t^2}, \tag{1}$$

where u is the displacement of particles of the medium, c_{ijkl} is the elastic stiffness tensor, and ρ is the mass density. The values of these constants we use in our calculations are listed in Table I.[10]

Solving the general equation, Eq. (1), can be extremely time consuming and unstable for some parameter ranges. If we restrict the solutions to be of a Rayleigh-type wave, which we are primarily interested in, the calculation can be greatly simplified. For the x propagation on the z surface, one can assume a solution[13]

$$\begin{pmatrix} u_x \\ u_z \end{pmatrix} \propto \begin{pmatrix} 1 \\ i\gamma \end{pmatrix} e^{-q\Omega z} e^{i(qx-\omega t)}, \tag{2}$$

where $q=\omega/v_s$ is the wave number and $\omega=2\pi f_s$ is the angular frequency. The SAW velocity and the SAW frequency are v_s and $f_s=v_s/\lambda_s$ with λ_s being the SAW wavelength, respectively. Ω satisfies the relation

$$(\rho v_s^2 - c_1 + c_{11}\Omega^2)(\rho v_s^2 - c_2 + c_1\Omega^2) + (c_1+c_3)^2 = 0 \tag{3}$$

and

$$\gamma = \frac{(c_1+c_3)\Omega}{\rho v_s^2 - c_1 + c_{11}\Omega^2}. \tag{4}$$

The coefficients c_1, c_2, and c_3 depend on the direction of the SAW propagation with respect to the crystal orientation and are given in Table II. One immediately notices from Eq. (3) that two of the four solutions of Ω are either with opposite signs, when Ω^2 is real, or complex conjugates, when Ω^2 is imaginary, of the other two solutions. The stress-free condition

$$\sigma_{iz} = \sum_{\kappa,l} c_{izkl}\frac{\partial u_k}{\partial x_l} = 0 \tag{5}$$

is imposed at the surface $z=0$. For a bulk crystal, this boundary condition leads to the following relation:

$$(\gamma_1+\Omega_1)(c_3 - c_{11}\gamma_2\Omega_2) - (\gamma_2+\Omega_2)(c_3 - c_{11}\gamma_1\Omega_1) = 0. \tag{6}$$

Here Ω_i and γ_i are the parameters corresponding to the two sets ($i=1$ and 2) of unrelated solutions of Eq. (3). In layered structures, the continuity of displacement fields, u_x and u_z, and stresses, σ_{xz} and σ_{zz}, is additionally imposed for each heterointerface, and thus Eq. (6) is modified. In our numerical procedure, Ω and γ are calculated for a given value of velocity using Eqs. (3) and (4). The velocity for which Eq. (6), or its counterpart for layered structures, is satisfied corresponds to the SAW velocity.

III. RESULTS AND DISCUSSION

A. Bulk materials

As the SAW dispersion in layered structures originates from the mismatch of the acoustic properties, we first examine the various acoustic waves on the bulk (100) surfaces of AlN, GaN, and γ-$LiAlO_2$. In Fig. 2, we show the angular dispersion of a SAW and the longitudinal and transverse bulk waves. A leaky mode is also found for γ-$LiAlO_2$. The wave propagation is in the direction making an angle θ from the [010] direction in the (100) plane. The polarization of the transverse bulk wave is normal to the surface for the mode denoted T_1 and in plane for the mode denoted T_2. The transverse bulk sound velocity generally sets the threshold for the appearance of guided modes as for velocities above which the surface waves can be scattered into the bulk wave. The elastic constants of AlN and GaN are roughly identical. As a

TABLE II. Coefficients c_1, c_2, and c_3 for the [010] and [001] propagations of surface waves. The coefficients are identical for the (100) surfaces of hexagonal and tetragonal crystals.

	c_1	c_2	c_3
[010] propagation	c_{66}	c_{11}	c_{12}
[001] propagation	c_{44}	c_{33}	c_{13}

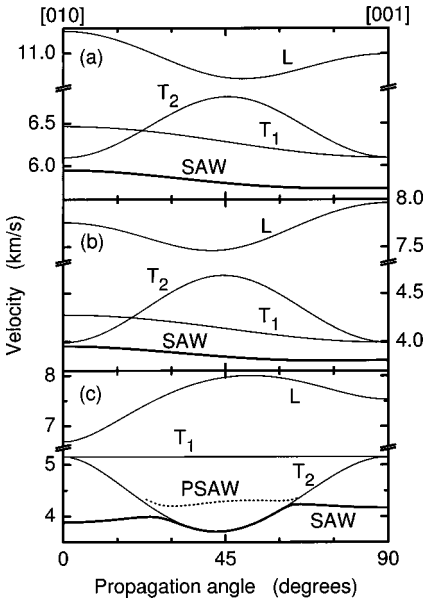

FIG. 2. Angular dispersion on the (100) surfaces of (a) AlN, (b) GaN, and (c) γ-$LiAlO_2$. The thick solid lines and the dotted line show the velocities of a SAW and a pseudo-SAW (PSAW), respectively. The velocities of the longitudinal bulk wave (L) and the transverse bulk waves (T_1 and T_2) are shown by the thin solid lines.

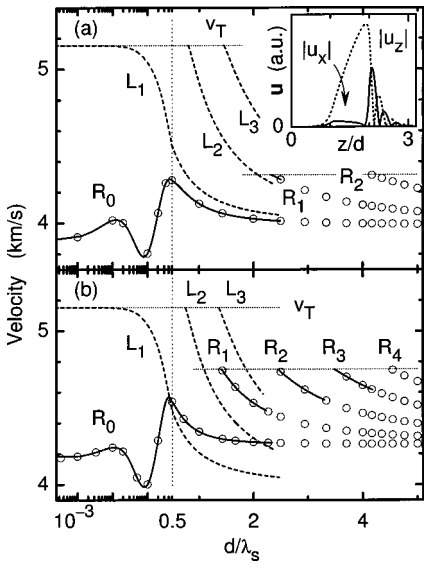

FIG. 3. Dispersion in the AlN/GaN/γ-$LiAlO_2$ heterostructure in the direction (a) along and (b) perpendicular to the c axis of the hexagonal bilayer film. The c axes of the bilayer film and the substrate are orthogonal to each other. The thicknesses of the AlN and GaN layers are assumed to be identical ($d_{\mathrm{AlN}}=d_{\mathrm{GaN}}=d$). The wavelength of the surface waves is λ_s. The modes denoted R_i and L_i are the ith Rayleigh-like and Love-like modes, respectively. Only the bottom three modes are shown for the Love-like modes. All the displacements are taken into account in the calculation for the solid and dashed lines. The short-wavelength limit of these dispersion curves is due to numerical instability. The wave is assumed to be sagittal for the circles. The horizontal-dotted lines indicate the threshold velocities of the guided modes. The threshold for the Love-like modes is the transverse bulk sound velocity v_T in γ-$LiAlO_2$. The inset in (a) shows the depth profile of the magnitude of the displacements u_x and u_z of the R_0 mode. The SAW propagation is along the c axis of the bilayer film and $d/\lambda_s=2.5$.

consequence, the difference of the dispersions in these two materials is approximately a scaling of the velocities by a factor of $\sim(6.15/3.23)^{1/2}\approx 1.4$. Interestingly, the velocity curves of the transverse bulk waves cross each other at $\theta=22°$ and 19° in AlN and GaN, respectively.

The behavior of the acoustic waves in γ-$LiAlO_2$ is similar to the one in cubic crystals such as GaAs. As a consequence of the lower crystal symmetry of the tetragonal structure of γ-$LiAlO_2$ in comparison to the cubic structure, the velocity minima and maxima are not located at $\theta=45°$. The deviations are, however, small. The SAW displacements are in the sagittal plane for the propagation along the [010] and [001] directions. When the SAW propagation is tilted from the [010] direction, the Rayleigh wave couples with a transverse bulk wave at $\theta\sim 27°$. The coupling results in the appearance of a leaky mode for $22°<\theta<66°$. The damping of the leaky mode reduces significantly when approaching $\theta=45°$ (not shown). However, $\theta=45°$ is again not the direction of the minimum damping.

B. Layered system

Figure 3 shows the dispersion of the Rayleigh-like modes (the solid lines and the circles), which are denoted R_i, and the Love-like modes (the dashed lines), which are denoted L_i, in an AlN/GaN/γ-$LiAlO_2$(100) heterostructure. The displacements are normally finite only within the sagittal plane for the Rayleigh-like modes, whereas the nonzero displacements are restricted to be within the plane parallel to the surface for the Love-like modes. The Love-like modes are usually piezoelectrically inactive. Consequently, interdigital transducers generally excite only the Rayleigh-like modes. The SAW propagation is (a) along the c axis and (b) perpendicular to the c axis of the bilayer film. The thicknesses of the AlN and GaN layers are assumed to be identical ($d_{\mathrm{AlN}}=d_{\mathrm{GaN}}=d$). The circles show the velocity of the Rayleigh-like modes estimated using the method based on Eqs. (2)–(6). The calculation that takes all the components of **u** into account (the solid and dashed lines) is limited to small values of d/λ_s due to numerical instability. The agreement between the two calculations indicates that the assumption of $u_y=0$ is justified for the Rayleigh-like modes.

Along the c axis of the bilayer film, SAWs propagate fastest in AlN and slowest in GaN. Therefore, with reducing λ_s, v_s is expected to decrease initially while the main part of the wave displacements shifts from the γ-$LiAlO_2$ substrate to the GaN layer. When λ_s is further reduced, v_s would then increase as the stiff AlN layer influences v_s. Although these trends are present, the numerically calculated dispersion reveals a much more complex behavior.

The most striking feature takes place in the short-wavelength regime. Instead of reaching the SAW velocity in AlN, v_s is significantly reduced when $\lambda_s\rightarrow 0$. The maximum SAW velocity is achieved at $d/\lambda_s=0.43$ and 0.41 for the propagation along and perpendicular to the c axis of the bilayer film, respectively. Moreover, new branches emerge in the dispersion one after the other with reducing λ_s. The SAW velocities associated with the newly generated modes decrease with reducing λ_s and appear to saturate at a common value. These characteristics resemble those of the guided modes in soft layers supported by hard substrates.[8,9] The distribution of the displacements reveals that the SAW modes

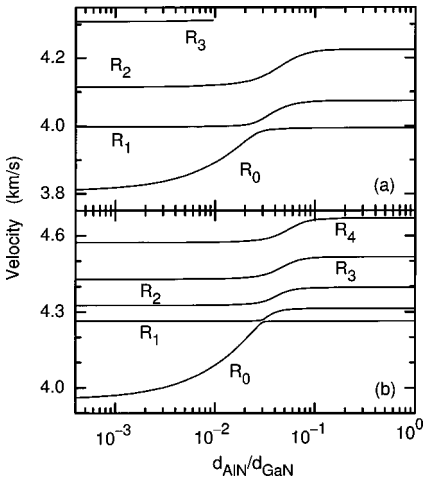

FIG. 4. Velocities of the guided Rayleigh-like modes R_i when the thickness of the AlN layer d_{AlN} is varied. The SAW wavelength is $\lambda_s/d_{\mathrm{GaN}}=0.2$. The SAW propagation is (a) along and (b) perpendicular to the c axis of the bilayer film. The transverse displacement u_y has been ignored for the calculation.

are strongly localized in the GaN layer in the short-wavelength regime, as shown in the inset of Fig. 3(a). The saturation velocity of the fundamental Rayleigh-like mode when $\lambda_s \rightarrow 0$ is, in fact, the velocity of the transversally polarized bulk acoustic wave T_1 of GaN (see Fig. 2(b)].[14] It is, therefore, indicated that the surface modes are expelled from the top AlN layer and accommodated in the adjacent GaN layer when the ordinary decay of the wave amplitude in the depth direction becomes energetically costly in the small λ_s regime. Such peculiar behavior originates from the extremely large velocity mismatch between AlN and GaN. The localization of the SAW displacements in the GaN layer is beneficial when SAWs are employed to modulate the electrical and optical properties in GaN–AlN quantum wells. The concentration of the SAW power results in an enhancement of the interaction between the SAW-induced piezoelectric fields and charged carriers in the GaN layer.

The velocity of guided modes at their emergence is generally given by a bulk transverse velocity in the substrate.[9] This is the case for the Love-like modes. However, the threshold velocity for the guided Rayleigh-like modes is lower than the bulk velocity. The threshold velocity in the latter case is found to correspond to a transition in which Ω^2 of the solution of Eq. (2) in γ-$LiAlO_2$ changes from complex numbers, in the small velocity regime, to real numbers, in the large velocity regime. The values of Ω in γ-$LiAlO_2$ for the velocities above the threshold contain a pure imaginary number. As the acoustic wave does not fully decay in the substrate, its confinement near the surface ceases to exist.

With reducing the thickness of the AlN barrier layer, the confined modes in the AlN/GaN/γ-$LiAlO_2$ "acoustic well" are expected to become the guided modes in the GaN/γ-$LiAlO_2$ heterostructure. This is confirmed as one finds in Fig. 4. Here, λ_s is chosen to be considerably small compared to $d_{\mathrm{GaN}}(\lambda_s/d_{\mathrm{GaN}}=0.2)$, guaranteeing a good confinement of the surface modes in the GaN layer. The transition from the "well mode" to the conventional surface mode takes place at $d_{\mathrm{AlN}}/d_{\mathrm{GaN}} \sim 10^{-2}$ for the fundamental Rayleigh-like mode R_0. The velocity of the R_0 mode when $d_{\mathrm{AlN}} \rightarrow 0$ is the SAW velocity in bulk GaN. The higher-order surface modes undergo the transition to guided modes at larger values of d_{AlN}. Similar results are found, irrespective of the direction of the SAW propagation.

Unlike the anomalous velocity observed in the short-wavelength regime, v_s is given by that of γ-$LiAlO_2$ in the limit of $\lambda_s \rightarrow \infty$. Nevertheless, the dispersion exhibits an additional velocity peak at $d/\lambda_s=0.012$ in Fig. 3. Moreover, we find that the minimum velocity in the layered system can be even smaller than the SAW velocity in bulk GaN. These anomalies are attributed to the bowing behavior in the dispersion. In GaN/γ-$LiAlO_2$ heterostructures, v_s was found to be the smallest at a wavelength away from the two extremes $\lambda_s=0$ and ∞.[10] This velocity bowing effect is responsible for the fact that the SAW velocity in the softest material of the layered system does not set the lower bound of v_s in AlN/GaN/γ-$LiAlO_2$ heterostructures. Similarly, the bowing effect of the reversed type is expected to have created the second velocity peak intermediate between two wavelength regimes, each of which is dominated by the GaN layer and the γ-$LiAlO_2$ substrate.

It should be noted that the elastic constants for γ-$LiAlO_2$ used in our calculations involve significantly large uncertainties. The experimentally observed SAW velocities in bulk γ-$LiAlO_2$(100) ($\approx$5.0 km/s both along the [010] and [001] directions[10]) are considerably larger than those obtained by the theory. Therefore, our numerical predictions need to be refined using accurate elastic constants for γ-$LiAlO_2$. Nevertheless, the main findings in the present paper are expected to be qualitatively unchanged. The elastic properties of the substrate do not contribute significantly to the SAW velocity in the short-wavelength regime, in which the localization phenomenon occurs. The velocity bowing effects in the long-wavelength regime are anticipated to remain important also after a correction of the elastic constants for γ-$LiAlO_2$. The effects are observed to be robust when the elastic constants are varied around the values presented in Table I. The velocity reduction due to the bowing effect was observed experimentally at least along the c axis of the overlayer in a GaN/γ-$LiAlO_2$ heterostructure.[10]

IV. CONCLUSION

In conclusion, the dispersion of the surface modes in AlN/GaN/γ-$LiAlO_2$ heterostructures has been numerically calculated. Both Rayleigh-like and Love-like modes are found to be squeezed into the GaN embedded layer instead of the AlN top layer in the short-wavelength regime. The expulsion from the top layer originates from the markedly fast sound propagation in AlN compared to that in the remaining components. The confinement effect is advantageous in controlling the operation of GaN-based devices by SAWs. The threshold velocity when guided Rayleigh-like modes emerge is less than the velocity of the transverse bulk wave in the substrate. We have also shown that the velocity bowing effects modify the dispersion to a significant extent.

The AlN/GaN/γ-$LiAlO_2$ heterostructures are thus predicted to be an interesting material system in which various unusual properties of SAWs are exhibited.

[1]H. Okano, N. Tanaka, Y. Takahashi, T. Tanaka, K. Shibata, and S. Nakano, Appl. Phys. Lett. **64**, 166 (1994).
[2]Y. Takagaki, P. V. Santos, E. Wiebicke, O. Brandt, H.-P. Schönherr, and K. H. Ploog, Appl. Phys. Lett. **81**, 2538 (2002).
[3]Y. Takagaki, O. Brandt, and K. H. Ploog, Jpn. J. Appl. Phys., Part 1 **42**, 1594 (2003).
[4]Y. Takagaki, T. Hesjedal, O. Brandt, and K. H. Ploog, Semicond. Sci. Technol. **19**, 256 (2004).
[5]O. Ambacher, J. Phys. D **31**, 2653 (1998).
[6]G. Bu, D. Ciplys, M. Shur, L. J. Schowalter, S. Schujman, and R. Gaska, Appl. Phys. Lett. **84**, 4611 (2004).
[7]C. Deger, E. Born, H. Angerer, O. Ambacher, M. Stutzmann, J. Hornsteiner, E. Riha, and G. Fischerauer, Appl. Phys. Lett. **72**, 2400 (1998).
[8]K. H. Choi, H. J. Kim, S. J. Chung, J. Y. Kim, T. K. Lee, and Y. J. Kim, J. Mater. Res. **18**, 1157 (2003).
[9]Y. Takagaki, P. V. Santos, E. Wiebicke, O. Brandt, H.-P. Schönherr, and K. H. Ploog, Phys. Rev. B **66**, 155439 (2002).
[10]Y. Takagaki, C. Hucho, E. Wiebicke, Y. J. Sun, O. Brandt, M. Ramsteiner, and K. H. Ploog, Phys. Rev. B **69**, 115317 (2004).
[11]P. Waltereit, O. Brandt, A. Trampert, H. T. Grahn, J. Menniger, M. Ramsteiner, M. Reiche, and K. H. Ploog, Nature (London) **406**, 865 (2000).
[12]Y. Takagaki, Y. J. Sun, O. Brandt, and K. H. Ploog, Appl. Phys. Lett. **84**, 4756 (2004).
[13]Love-type waves can also be calculated by taking only $u_y(x,z)$ into account.
[14]To be precise, v_s of the R_0 mode in the short-wavelength regime is slightly lower (less than 1% at $d/\lambda_s=10$) than the bulk transverse velocity of GaN. It is not clear, at present, if v_s is eventually given by the SAW velocity in AlN in the limit of $\lambda_s=0$.